

Survey of the (${}^9\text{Be}, {}^6\text{He}$) reaction on ${}^9\text{Be}$, ${}^{10}\text{B}$, ${}^{11}\text{B}$, and ${}^{12}\text{C}$

L. M. Comer, E. L. Reber, K. W. Kemper, and D. Robson

Department of Physics, Florida State University, Tallahassee, Florida 32306

J. D. Brown

Joseph Henry Laboratories, Princeton University, Princeton, New Jersey 08544

T. L. Talley

Theoretical Division, Los Alamos National Laboratory, Los Alamos, New Mexico 87545

(Received 2 October 1991)

Elastic scattering and (${}^9\text{Be}, {}^6\text{He}$) reaction data have been taken at a ${}^9\text{Be}$ bombarding energy of 40 MeV. The reaction data are consistent with (${}^9\text{Be}, {}^6\text{He}$) being a direct ${}^3\text{He}$ cluster transfer, so that population of $T_{>} = 3/2$ final states from $T = 0$ targets is unlikely. Contributions to the elastic scattering arising from the identity of the target and projectile have been calculated. Large deviations from standard optical model calculations do not occur until scattering angles are larger than 90° c.m.

PACS number(s): 25.70.Hi, 25.70.Bc

I. INTRODUCTION

The (${}^9\text{Be}, {}^6\text{He}$) reaction is a somewhat unique three-particle transfer reaction because it can populate states of isospin $T_{<}$ and $T_{>}$ in the final nucleus for a $T = 0$ target, unless it proceeds as a ${}^3\text{He}$ cluster transfer, in which case only $T_{<}$ states are populated. The present survey of the (${}^9\text{Be}, {}^6\text{He}$) reaction was motivated by the need for a three-particle transfer reaction that can populate the proposed $T_{>}$ states observed [1] by the (p, π^+) reaction in light nuclei. The only previously reported data [2] on the (${}^9\text{Be}, {}^6\text{He}$) reaction is a spectrum of the ${}^9\text{Be}({}^9\text{Be}, {}^6\text{He}){}^{12}\text{C}$ reaction taken at a bombarding energy of 26 MeV. No absolute cross sections were given although it was commented that the cross section was appreciable and that the relative population of the states implied a direct reaction mechanism.

In the present work, angular distributions have been measured for the (${}^9\text{Be}, {}^6\text{He}$) reaction on the targets ${}^9\text{Be}$, ${}^{10}\text{B}$, ${}^{11}\text{B}$, and ${}^{12}\text{C}$ at a bombarding energy of 40 MeV. This energy was chosen because it is in the energy region where previous extensive studies of ${}^9\text{Be}$ elastic scattering have been carried out and the (${}^9\text{Be}, {}^6\text{He}$) transitions to the isolated low-lying states are well angular momentum matched. Limited elastic scattering angular distributions were also taken. Previously reported ${}^9\text{Be} + {}^9\text{Be}$ elastic data [3] are shown to have their angle scale shifted by 5° . The present analysis of the ${}^9\text{Be} + {}^9\text{Be}$ elastic data includes the contribution arising from the identity of the projectile and target. The transfer data were compared to finite-range distorted-wave-Born-approximation (FRDWBA) calculations to extract spectroscopic factors for ${}^3\text{He}$ cluster transfer.

II. EXPERIMENTAL PROCEDURE

A BeH^- beam was extracted from an inverted sputter source and accelerated by the Florida State University

tandem Van de Graaff to 40 MeV after being stripped to ${}^9\text{Be}^{+4}$. The typical beam current on target was 50 electrons nA. The ${}^9\text{Be}$, ${}^{10}\text{B}$ (93%), ${}^{11}\text{B}$ (98%), and ${}^{12}\text{C}$ (natural) targets were self-supporting and had thicknesses of $100 \mu\text{g}/\text{cm}^2$ except for ${}^{12}\text{C}$ which was $200 \mu\text{g}/\text{cm}^2$. Three standard $\Delta E \times E$ silicon detector telescopes were used with the two most forward telescopes having silicon surface barrier ΔE detectors of thickness $40 \mu\text{m}$ and the third one having a thickness of $25 \mu\text{m}$. All three Si(Li) E detectors were $5000 \mu\text{m}$ thick. The individual particle groups were sorted on line into energy spectra. The detectors subtended a polar angle of 0.6° . A stationary silicon detector was used throughout the run to monitor the charge integration and target condition. The errors in the absolute cross sections for the (${}^9\text{Be}, {}^6\text{He}$) reactions were determined to be $\pm 18\%$ by comparing to the elastic scattering results taken simultaneously, as will be discussed later.

During the course of the analysis it became obvious that very forward angle ${}^9\text{Be}({}^9\text{Be}, {}^6\text{He}){}^{12}\text{C}$ data would be necessary for understanding the reaction mechanism. To take these data, an Al foil that stopped ${}^9\text{Be}$ but allowed the ${}^6\text{He}$ to pass through was placed in front of the counter telescope. It was possible to gather data into 2° laboratory with this arrangement.

Typical (${}^9\text{Be}, {}^6\text{He}$) spectra for the four targets are shown in Fig. 1. There were no identifiable ${}^{15}\text{O}$ states populated in the ${}^{12}\text{C}({}^9\text{Be}, {}^6\text{He})$ reaction at the six angles where data were taken. The yield between the dashed lines in this spectrum corresponds to a cross section of $4 \mu\text{b}/\text{sr}$. Figure 2 is a comparison between ${}^9\text{Be}({}^9\text{Be}, {}^6\text{He}){}^{12}\text{C}$ and ${}^9\text{Be}({}^6\text{Li}, t){}^{12}\text{C}$ spectra [4]. The primary difference in the two reactions is that (${}^9\text{Be}, {}^6\text{He}$) populates the 14.08 (4^+) state much more weakly than does (${}^6\text{Li}, t$), relative to the lower lying states. The ${}^9\text{Be}({}^9\text{Be}, {}^6\text{He}){}^{12}\text{C}$ spectrum published earlier [2] for a ${}^9\text{Be}$ bombarding energy of 26 MeV has the same features as

the one shown here. Both reactions populate the 7.65 and 0.0 MeV, 0^+ states with about equal intensity. The comparison between $^{11}\text{B}(^9\text{Be}, ^6\text{He})^{14}\text{N}$ and $^{11}\text{B}(^6\text{Li}, t)^{14}\text{N}$ spectra [5] in Fig. 3 again shows that the two reactions populate the same state or groups of states. The sparse population of ^{13}N states in the $^{10}\text{B}(^9\text{Be}, ^6\text{He})$ reaction makes it difficult to get a detailed comparison with the $^{10}\text{B}(^6\text{Li}, t)$ reaction [6], but the strong states observed at 9 and 10.36 MeV are observed in both reactions. The small cross section for populating states in ^{15}O by the $^{12}\text{C}(^9\text{Be}, ^6\text{He})$ reaction was somewhat of a surprise since the angular momentum mismatch is similar to that of $^{12}\text{C}(^6\text{Li}, t)$ for 5 MeV excitation in ^{15}O and it was ex-

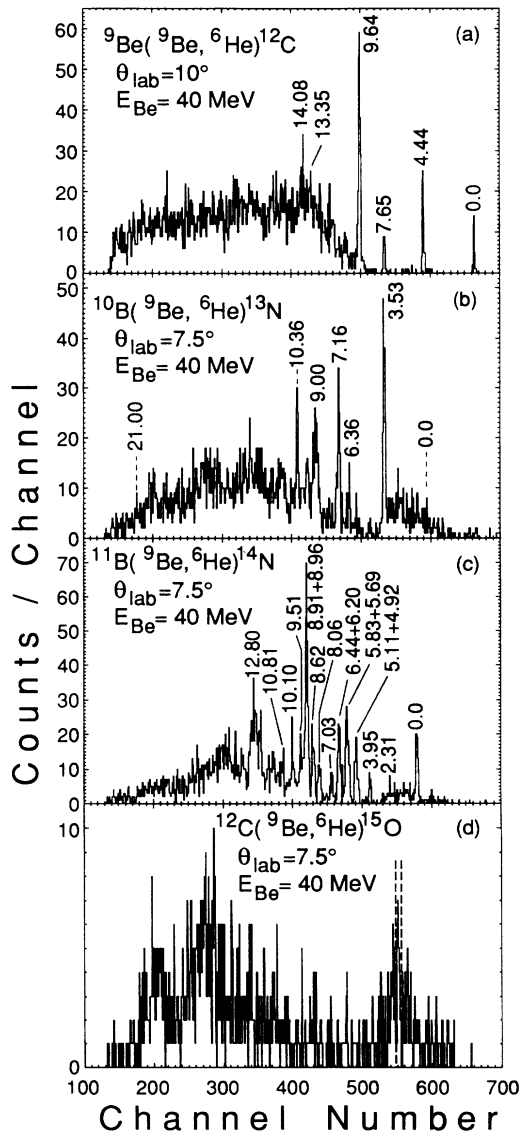


FIG. 1. Typical spectra for the $(^9\text{Be}, ^6\text{He})$ reaction on the targets ^9Be , ^{10}B , ^{11}B , and ^{12}C . The location of 21 MeV in excitation in ^{13}N is shown. Also, the dashed lines in the $^{12}\text{C}(^9\text{Be}, ^6\text{He})$ spectrum show the expected location of the ^{15}O ground state. No distinct peaks were observed at any angle in this reaction.

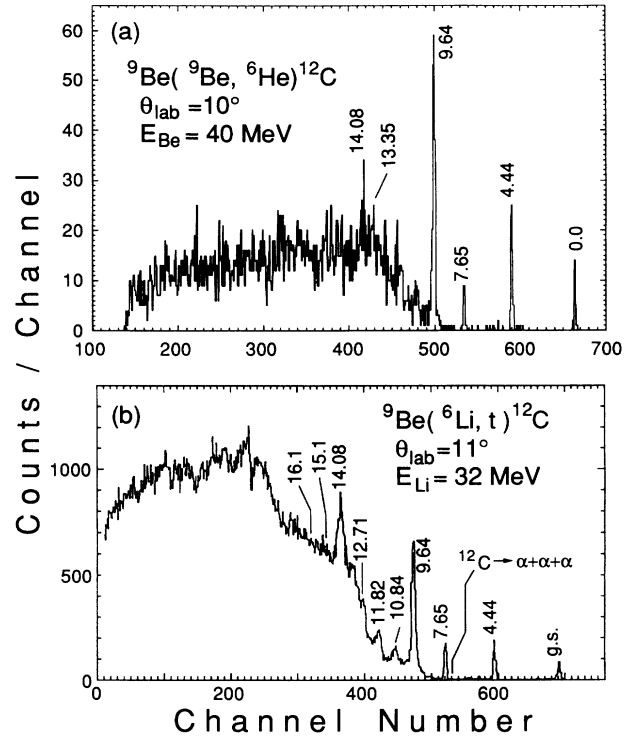


FIG. 2. Comparison of $^9\text{Be}(^9\text{Be}, ^6\text{He})^{12}\text{C}$ and $^9\text{Be}(^6\text{Li}, t)^{12}\text{C}$ [4] spectra.

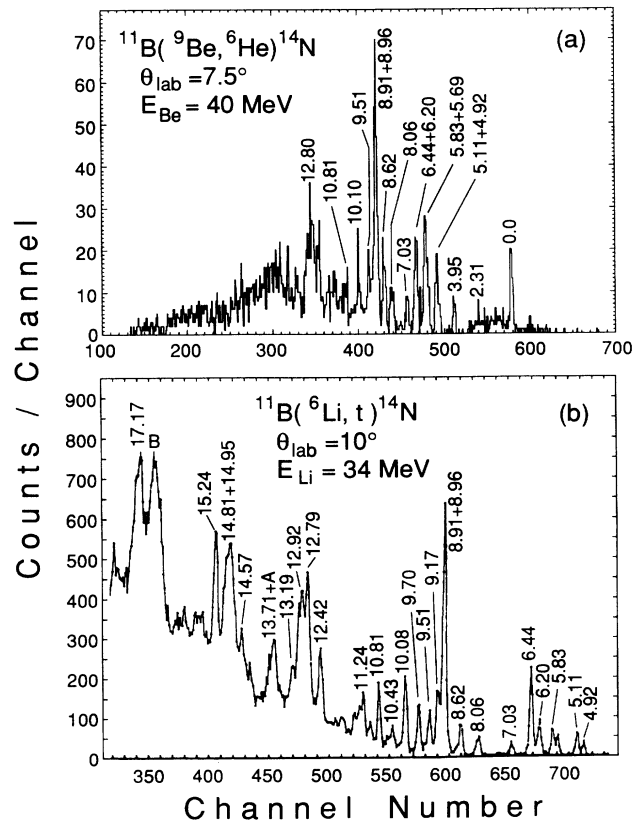


FIG. 3. Comparison of $^{11}\text{B}(^9\text{Be}, ^6\text{He})^{14}\text{N}$ and $^{11}\text{B}(^6\text{Li}, t)^{14}\text{N}$ (Ref. [5]) spectra. The detectors used in Ref. [5] were not thick enough to stop the tritons populating the first three states in ^{14}N .

pected that both the 5.24 MeV ($\frac{5}{2}^+$) and 10.46 MeV ($\frac{9}{2}^+$) states would be populated by the (${}^9\text{Be}, {}^6\text{He}$) reaction.

III. RESULTS

A. Elastic scattering

It was initially assumed that previously measured elastic ${}^9\text{Be} + {}^9\text{Be}$ scattering [3] could be used to provide both absolute cross sections for the present ${}^9\text{Be}({}^9\text{Be}, {}^6\text{He}){}^{12}\text{C}$ reaction data and optical model parameters for the generation of the distorted waves in the finite-range distorted-wave-Born-approximation (FRDWBA) calculations. However, limited elastic scattering data taken simultaneously with the reaction data did not agree with that previously published [3], making the taking of elastic scattering data on all targets for the angular range between about 10° and 60° c.m. necessary. Only forward angle data were taken because cluster transfer contributions have been shown to be present at larger angles [7, 8] for ${}^9\text{Be}$ scattering from light targets.

Good agreement was found for ${}^9\text{Be} + {}^{12}\text{C}$ scattering with both the data and calculations of Mateja *et al.* [8] and with elastic scattering calculations performed with the systematic optical model parameters from Jarczyk *et al.* [7]. The structure in the data for ${}^9\text{Be} + {}^9\text{Be}$ agree well with calculations performed with parameters from Ref. [7]. The work of Omar *et al.* [3] are consistent with the present results and those of Ref. [7], if it is assumed that their starting angle for the elastic scattering angular distribution figures should be 0° c.m. rather than 5° c.m. The present ${}^9\text{Be} + {}^9\text{Be}^*$ (2.43 MeV) inelastic scattering data are also in good agreement with that of Omar *et al.* [3], where their angle scale in fact starts at 0° c.m.

A concern in the description of the ${}^9\text{Be} + {}^9\text{Be}$ scattering is whether the identity of the target and projectile needs to be taken into account for the forward angles measured here. It is argued in Ref. [3] that the strong absorption found in ${}^9\text{Be}$ elastic scattering greatly reduces the importance of symmetrization at forward angles. The optical model code HERMES [9] was modified to include the symmetrization term [10]. The calculation with the 127.7 MeV potential of Table I (taken from Ref. [3]) with symmetrization not included is shown plotted as the ratio-to-Rutherford cross section in Fig. 4, and with symmetrization included as the ratio-to-Mott cross section also in Fig. 4. As can be seen, the identity of

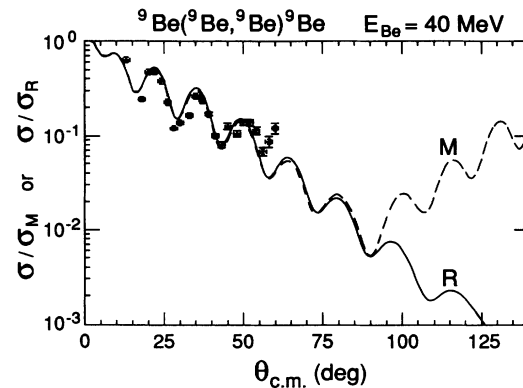


FIG. 4. Elastic ${}^9\text{Be} + {}^9\text{Be}$ scattering given as the ratio-to-Rutherford or as the ratio-to-Mott. The ratio-to-Mott calculated cross section includes the contribution to the scattering arising from the identity of the target and projectile.

the target and projectile does not have to be taken into account for scattering into angles less than 90° c.m.

The absolute cross sections for the elastic scattering angular distributions for the ${}^{10}\text{B}$, ${}^{11}\text{B}$, and ${}^{12}\text{C}$ targets were determined by comparing the five or so most forward angle data points in each angular distribution to optical model calculations carried out with the published parameters of Refs. [7,8]. In addition, the cross sections were determined from the measured detector solid angles, integrated beam current, and the target thickness obtained from a crystal thickness monitor. The two absolute cross section methods agreed to within 18%, which is then taken to be the uncertainty in the absolute cross section determinations.

To determine the optical model parameters needed for generating the distorted waves in the analysis of the transfer data, optical model searches with Woods-Saxon real and imaginary volume potentials were carried out with the ${}^9\text{Be} + {}^{12}\text{C}$ parameters of Mateja *et al.* [8] used as starting values for the targets ${}^9\text{Be}$, ${}^{10}\text{B}$, and ${}^{11}\text{B}$. It was not possible to find a satisfactory fit to all four sets of elastic data when the parameters of Omar *et al.* [3] were used as starting values, whereas it was possible with the Mateja *et al.* [8] parameters. The resulting potential sets are given in Table I and the calculations and data are shown in Fig. 5.

TABLE I. Woods-Saxon optical model parameters obtained from the present elastic scattering data. A volume Woods-Saxon imaginary potential was used.

Target	V (MeV)	r_r (fm) ^a	a_r (fm)	W (MeV)	r_I (fm) ^a	a_I (fm)
${}^9\text{Be}$	32.2	1.44	1.19	13.0	2.88	0.60
${}^{10}\text{B}$	53.7	1.22	1.19	12.1	2.88	0.48
${}^{11}\text{B}$	29.2	1.02	1.50	8.76	2.77	0.62
${}^{12}\text{C}$	33.7	1.84	0.92	6.52	2.88	0.48
${}^9\text{Be}^b$	127.7	1.62	0.73	16.4	2.61	0.76

^a $R_x = r_x A_T^{1/3}$; $R_c = 2.4 A_T^{1/3}$.

^b Potential geometry taken from Ref. [3].

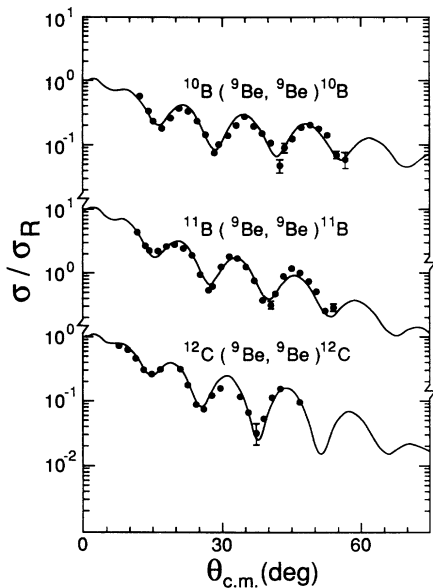


FIG. 5. Elastic scattering data and optical model calculations for the systems shown. The parameters are those given in Table I.

B. The (⁹Be,⁶He) reaction

The approach taken in the present work to determine if the (⁹Be,⁶He) reaction can be considered a ³He cluster transfer is to compare relative spectroscopic factors obtained from finite-range distorted-wave-Born-approximation calculations (FRDWBA) with those obtained from (⁶Li,t) and the theoretical values of Kurath and Millener [11], where available. The analysis concentrated on the ⁹Be(⁹Be,⁶He)¹²C and ¹¹B(⁹Be,⁶He)¹⁴N reactions since both of these had large enough cross sections to isolated states to allow comparisons between calculated and measured angular distributions. It was assumed that the ³He cluster had the quantum numbers 2N + L = 3 for the ³He + ⁶He → ⁹Be bound state as well as for positive parity states in ¹²C formed by ³He + ⁹Be. For the transition to the 3⁻, 9.64 MeV state in ¹²C, it was assumed that 2N + L = 4. Woods-Saxon potential wells were used for the bound states each with a radius parameter of 1.23 fm and diffuseness of 0.65 fm. These values are typical for these light systems [12]. The entrance channel distorted waves were generated using the optical potentials from Table I. The ⁶Li + ¹²C potential set IV from Table I of Vineyard *et al.* [13] was used for the ⁶He exit channel. A recent survey [14] of ⁶He elastic

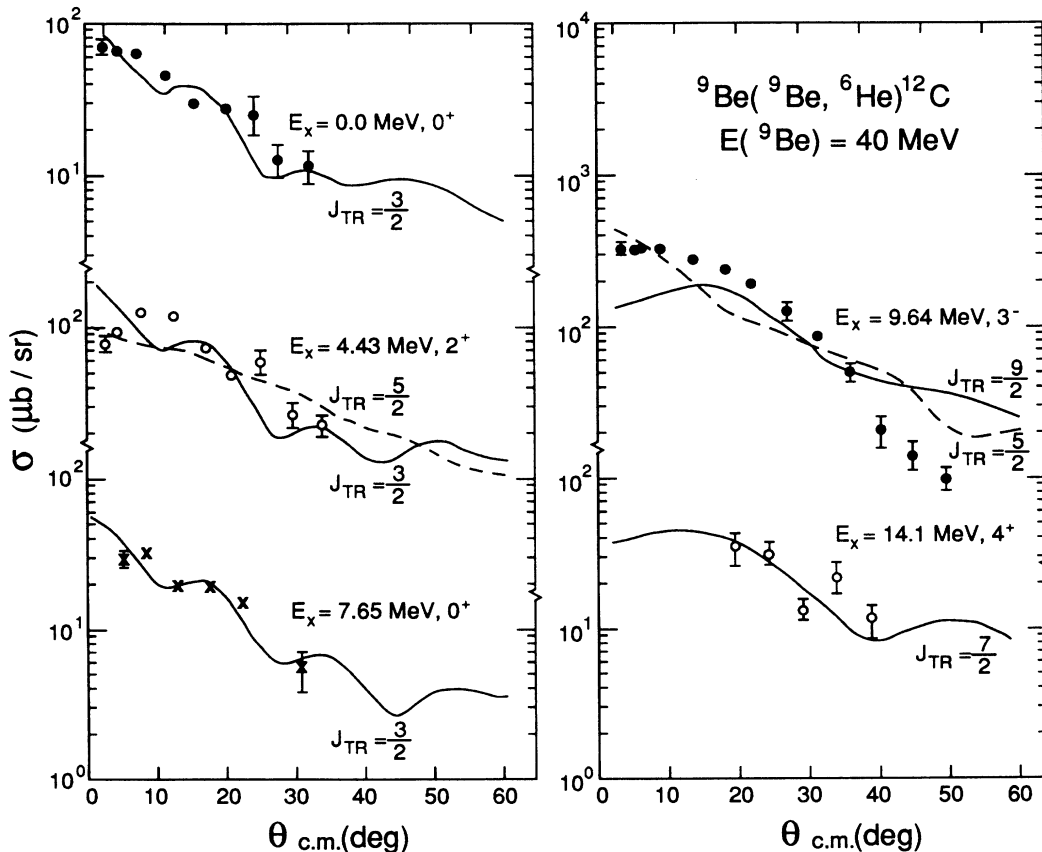


FIG. 6. Angular distribution data and finite-range DWBA calculations for the ⁹Be(⁹Be,⁶He)¹²C reaction. The total angular momentum transfer assumed for the ⁹Be + ³He → ¹²C transfer is shown.

scattering is consistent with this assumption.

The spectroscopic factor products for the transfer transitions were obtained by comparing the DWUCK5 [15] finite-range DWBA calculations to the data. The two quantities are related by the expression

$$\sigma_{\text{exp}} = \frac{2J_f + 1}{2J_i + 1} C^2 S_1 C^2 S_2 \sigma_{\text{DWUCK5}}, \quad (1)$$

where J_f and J_i are the initial and final state spins and $C^2 S_1$ and $C^2 S_2$ are the projectile and target ${}^3\text{He}$ cluster spectroscopic factors. This expression assumes that the ${}^3\text{He}$ cluster in the final state has only one value of N , L , and J . Attempts were not made to determine relative contributions from the different orbital angular momenta transfers in transitions that allow more than one, because the limited scope of the data do not justify such fitting.

The calculated and experimental angular distributions for the ${}^9\text{Be}({}^9\text{Be}, {}^6\text{He}){}^{12}\text{C}$ transitions are shown in Fig. 6. Since the ground-state transition can only take place by $J_{\text{tr}} = \frac{3}{2}$, it provides a more stringent test of the calculations than do the other transitions. The FRDWBA calculations showed a rather steep rise for angles smaller than 12° c.m. As can be seen, the calculations give a good reproduction of these data. The extracted spectroscopic factor products $C^2 S_1 C^2 S_2$ are given in Table II along with the values of N , L , and J_{tr} assumed for the ${}^3\text{He}$ cluster bound to ${}^9\text{Be}$ to form ${}^{12}\text{C}$. The fact that these products are close to one shows that the DWBA calculations predict the absolute magnitude of the cross sections to within a factor of 2 or 3, suggesting that the cluster transfer description of (${}^9\text{Be}, {}^6\text{He}$) is reasonable. This result is similar to that found by Hamill and Kunz [16] for (${}^6\text{Li}, t$). They showed that the absolute magnitude of the (${}^6\text{Li}, t$) reaction is well described by exact finite-range DWBA calculations, while the (α, p) reaction is underpredicted by at least a factor of 100. Table II also contains the spectroscopic factor product for each of the transitions divided by the ground-state product so that comparisons can be made with the previously published (${}^6\text{Li}, t$) results [4] and also with the theoretical values of Kurath and Millener [11]. As can be seen, the

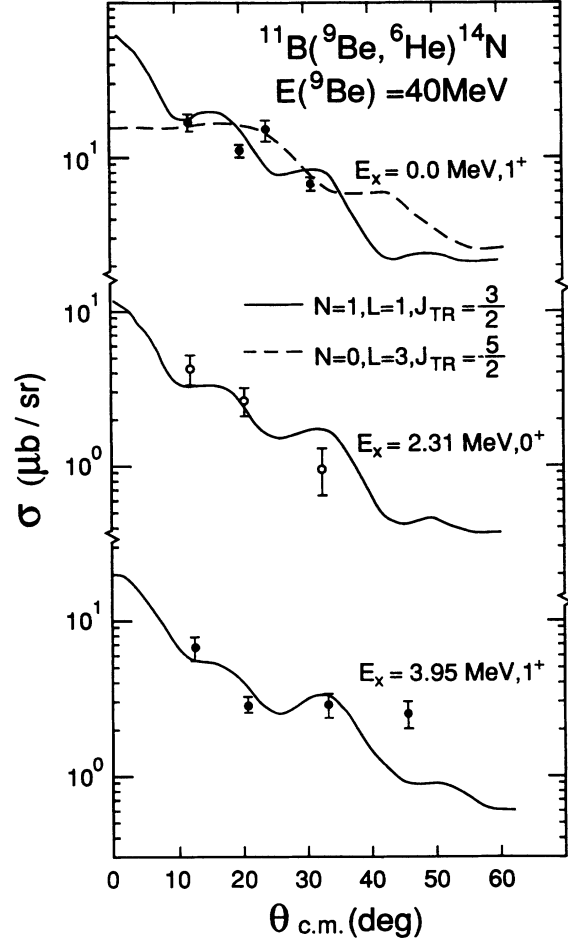


FIG. 7. Data and FRDWBA calculations for the transitions to the first three states in ${}^{14}\text{N}$.

different values are in qualitative agreement, supporting the assumption of ${}^3\text{He}$ cluster transfer for the (${}^9\text{Be}, {}^6\text{He}$) reaction.

Because many of the transitions that occur in the ${}^{11}\text{B}({}^9\text{Be}, {}^6\text{He}){}^{14}\text{N}$ reaction are to unresolved groups of

TABLE II. Product of cluster spectroscopic strengths for ${}^9\text{Be}({}^9\text{Be}, {}^6\text{He}){}^{12}\text{C}$.

E_x	J^π	N	L	$2J_{\text{tr}}$	$C^2 S_1 C^2 S_2$	$\frac{C^2 S_1 C^2 S_2}{(C^2 S_1 C^2 S_2)_{\text{g.s.}}}$	$({}^6\text{Li}, t)^a$	KM ^b
0.0	0^+	1	1	3	4.1	1.0	1.0	1.0
4.43	2^+	1	1	3	1.2	0.29	0.05	0.21
		0	3	5	5.0	1.22	0.68	
7.65	0^+	1	1	3	1.7	0.41	1.67	
9.64	3^-	1	2	5	1.7	0.41	0.43	
		0	4	9	7.5	1.83	1.85	
14.08	4^+	0	3	5	1.4	0.34	0.60	0.13

^aReference [4].

^bReference [14].

TABLE III. Product of cluster spectroscopic factors for the $^{11}\text{B}(^9\text{Be}, ^6\text{He})^{14}\text{N}$ reaction.

E_x	J^π	N	L	$2J_{tr}$	$C^2S_1C^2S_2$	$\frac{C^2S_1C^2S_2}{(C^2S_1C^2S_2)_{g.s.}}$	KM ^a
0.0	1^+	1	1	3	0.24	1.00	1.00
		0	3	5	0.87	(1.00) ^b	(1.00)
2.31	0^+	1	1	3	0.14	0.58 (0.16)	6.14 (0.81)
3.95	1^+	1	1	3	0.10	0.42 (0.12)	0.67 (0.09)

^aReference [14].

^bValues in parentheses are ratios found by using the $N = 0$, $L = 3$ experimental spectroscopic factor product of 0.87 or the square of the F -wave ground-state parentage amplitude of Ref. [14].

states it is only possible to carry out a detailed analysis of the transitions to the first three states in ^{14}N . For the transitions to the 1^+ , 0.0 and 3.95 MeV states, both $N = 1$, $L = 1$ and $N = 0$, $L = 3$ transfer occurs while only $N = 1$, $L = 1$ occurs for the transition to the 0^+ , 2.31 MeV state. Ground-state calculations for both $L = 1$ and $L = 3$ transfers are shown, while for the other two transitions only $L = 1$ are shown in Fig. 7. The extracted spectroscopic factor products are given in Table III. The ratio of the experimental spectroscopic factors relative to that for the ground-state transition shows that the calculations of Kurath and Millener overpredict the spectroscopic strength to the 0^+ , 2.31 MeV state by a factor of 5 but are in good agreement with the data for the 1^+ , 3.95 state. The numbers to be compared in Table III are those in brackets since Kurath and Millener (KM) predict that the $L = 3$ ground-state strength is seven times greater than that for $L = 1$. The experimental ratio of the $N = 0$, $L = 3$ ground-state strength of ^{14}N to the $N = 1$, $L = 1$ ground-state strength of ^{12}C is 0.29, while the KM prediction is 0.21. These results are again, consistent with ^3He cluster transfer for the $(^9\text{Be}, ^6\text{He})$ reaction.

The lack of population of the ^{13}N ground state in the $^{10}\text{B}(^9\text{Be}, ^6\text{He})^{13}\text{N}$ reaction was somewhat of a sur-

prise since the KM calculation indicated a spectroscopic strength comparable to that for $^9\text{Be} + ^3\text{He} \rightarrow ^{12}\text{C}$ and $^{11}\text{B} + ^3\text{He} \rightarrow ^{14}\text{N}$ for the system $^{10}\text{B} + ^3\text{He} \rightarrow ^{13}\text{N}$. The ground state is also weakly populated in the $^{10}\text{B}(^6\text{Li}, t)^{13}\text{N}$ reaction [6]. A DWBA calculation of the yield expected for the ground-state transition with the Kurath-Millener spectroscopic strength would have yielded a peak of height 10 counts in the spectrum shown in Fig. 1, and an integrated peak yield of 30 counts. The experimental result is about a factor of 3 below this value. The angular distribution for the $^{10}\text{B}(^9\text{Be}, ^6\text{He})^{13}\text{N}$ transition to the $\frac{5}{2}^+$, $\frac{3}{2}^-$ doublet at 3.5 MeV in ^{13}N is shown in Fig. 8. A DWBA calculation assuming that the $\frac{5}{2}^+$ state is populated, is shown. The extracted spectroscopic factor product is 0.51.

No conclusion can be reached about the $^{12}\text{C}(^9\text{Be}, ^6\text{He})^{15}\text{O}$ reaction since no discrete peaks were observed. The ground-state cross section would be 4 $\mu\text{b}/\text{sr}$ if it is assumed that the region between the dashed lines in Fig. 1 corresponds to its population. This experimental cross section is a factor of 5 smaller than one predicted from DWBA calculations, with the Kurath-Millener $^{12}\text{C} + ^3\text{He} \rightarrow ^{15}\text{O}$ spectroscopic strength.

IV. CONCLUSIONS

The $(^9\text{Be}, ^6\text{He})$ reaction has been shown to be consistent with ^3He cluster transfer, thus making its usefulness for probing $T_>$ strength limited when beginning with $T = 0$ targets. The absolute magnitude of this cross section is 2-3 times smaller than that for the corresponding $(^6\text{Li}, t)$ reaction. This difference is consistent with the factor of 4 smaller spectroscopic factor for $^9\text{Be} \rightarrow ^6\text{He} + ^3\text{He}$ (Ref. [14]) when compared with that for $^6\text{Li} \rightarrow t + ^3\text{He}$ (Ref. [17]). The absolute magnitude of the $(^9\text{Be}, ^6\text{He})$ cross sections seems to be reproduced by exact finite-range DWBA calculations. The small experimental cross section for the $^{12}\text{C}(^9\text{Be}, ^6\text{He})^{15}\text{O}$ reaction was unexpected when compared with the other observed cross sections.

The relative spectroscopic factors obtained for the $^9\text{Be}(^6\text{Li}, t)^{12}\text{C}$ and $^9\text{Be}(^9\text{Be}, ^6\text{He})^{12}\text{C}$ reactions are within a factor of 2 of each other for the dominant L transfers except for the transition to the 7.65 MeV 0^+ state. The extreme forward angle $(^9\text{Be}, ^6\text{He})$ data taken are shown to yield a signature of the J_{tr} of the transition. The

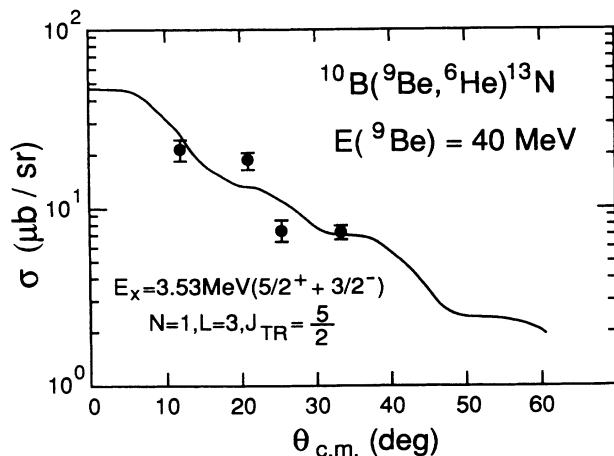


FIG. 8. Data and FRDWBA calculations to the doublet at 3.53 MeV in ^{13}N . The calculation assumes that the $\frac{5}{2}^+$ state is mainly populated.

Kurath-Millener spectroscopic factors are in good agreement with those obtained with the (${}^9\text{Be}, {}^6\text{He}$) reaction.

The elastic scattering of ${}^9\text{Be}$ was found to be in good agreement with previous measurements except for the case of ${}^9\text{Be} + {}^9\text{Be}$. In this case, the previous data [3] must be shifted forward by 5° c.m. The symmetry of the

${}^9\text{Be} + {}^9\text{Be}$ system does not affect the elastic scattering for angles less than 90° c.m.

This work was supported in part by the Department of Energy, National Science Foundation, and the State of Florida.

-
- [1] E. Korkmaz, S.E. Vigdor, W.W. Jacobs, T.G. Throwe, L.C. Bland, M.C. Green, P.L. Jolivet, and J.D. Brown, *Phys. Rev. C* **40**, 813 (1989); S.M. Aziz, A.D. Bacher, L.C. Bland, G.T. Emery, W.W. Jacobs, E. Korkmaz, H. Nann, P.W. Park, J. Templon, P.L. Walden, and G.M. Huber, *Bull. Am. Phys. Soc.* **32**, 1062 (1987); S.M. Aziz, Ph.D. thesis, Indiana University, 1988.
- [2] N.I. Venikov, Yu.A. Glukhov, V.I. Man'kov, B.G. Novatskii, A.A. Ogloblin, S.B. Sakuta, D.N. Stepanov, V.N. Unezhev, V.I. Chuev, and N.I. Chumakov, *Yad. Fiz.* **22**, 924 (1975) [*Sov. J. Nucl. Phys.* **22**, 481 (1976)].
- [3] A.R. Omar, J.S. Eck, J.R. Leigh, and T.R. Ophel, *Phys. Rev. C* **30**, 896 (1984).
- [4] X. Aslanoglou and K.W. Kemper, *Phys. Rev. C* **34**, 1649 (1986).
- [5] M.E. Clark and K.W. Kemper, *Nucl. Phys.* **A425**, 185 (1984).
- [6] C.H. Holbrow, H.G. Bingham, R. Middleton, and J.D. Garrett, *Phys. Rev. C* **9**, 902 (1974).
- [7] L. Jarczyk, J. Okolowicz, A. Strzalkowski, K. Bodek, M. Hugi, J. Lang, R. Muller, and E. Ungricht, *Nucl. Phys.* **A316**, 139 (1979).
- [8] J.F. Mateja, A.D. Frawley, P.B. Nagel, and L.A. Parks, *Phys. Rev. C* **20**, 176 (1979).
- [9] J. Cook, *Comput. Phys. Commun.* **31**, 363 (1984).
- [10] R. Bass, *Nuclear Reactions with Heavy Ions* (Springer-Verlag, Berlin, 1980), p. 13.
- [11] D. Kurath and D.J. Millener, *Nucl. Phys.* **A238**, 269 (1975).
- [12] K.-I. Kubo and M. Hirata, *Nucl. Phys.* **A187**, 186 (1972).
- [13] M.F. Vineyard, J. Cook, K.W. Kemper, and M.N. Stephens, *Phys. Rev. C* **30**, 916 (1984).
- [14] R.J. Smith, J.J. Kolata, K. Lamkin, A. Morsad, K. Ashktorab, F.D. Becchetti, J.A. Brown, J.W. Janecke, W.Z. Liu, and D.A. Roberts, *Phys. Rev. C* **43**, 761 (1991).
- [15] DWUCK5, P.D. Kunz, University of Colorado (unpublished).
- [16] J.J. Hamill and P.D. Kunz, *Phys. Lett.* **129B**, 5 (1983).
- [17] M.F. Werby, M.B. Greenfield, K.W. Kemper, D.L. McShan, and S. Edwards, *Phys. Rev. C* **8**, 106 (1973).